



Facultad de Ciencias

Sección de Física

Trabajo de Fin de Grado

Efecto Casimir

Alejandro Martín Gutiérrez

Tutor: **Dr. Daniel Alonso Ramírez**

July 2018

Abstract

En este trabajo presentamos una revisión bibliográfica del Efecto Casimir. Este fenómeno se produce debido a las fluctuaciones cuánticas del vacío. Se puede representar como una fuerza, atractiva o repulsiva. Estudiaremos una introducción al origen de este efecto descubierto por H.B.G. Casimir. A continuación, haremos un cálculo del Efecto Casimir para unas placas plano-paralelas, dándose una corrección térmica. También, reproduciremos el cálculo en el caso de una placa frente a una esfera y una esfera entre dos placas plano-paralelas. En el siguiente apartado, daremos una introducción a la Teoría Cuántica de Campos para determinar el Efecto Casimir en un campo escalar real. Después, comentaremos el primer experimento, hecho por Lamoreaux en 1996, que consiguió medir con suficiente precisión el Efecto Casimir. Para acabar, haremos un análisis de la magnitud del Efecto Casimir en los casos que hemos estudiado.

Contents

1	Introduction	1
1.1	Objectives and Methodology	1
1.2	The origin of the Casimir Effect	1
1.2.1	Quantum Vacuum	2
2	Casimir Effect	4
2.1	Plate-Plate configuration.	5
2.1.1	Attractive Force	5
2.1.2	Repulsive Force	8
2.1.3	Temperature correction.	9
2.2	Plate-Sphere configuration	12
2.3	Plate-Sphere-Plate configuration	15
2.4	Scalar Field Theory	16
2.4.1	A brief introduction of Quantum Field Theory	16
2.4.2	Local description of Casimir effect	17
2.4.3	Casimir effect with cutoff regularization	19
2.4.4	Casimir effect with Abel-Plana formula	21
3	Experimental demonstration	23
4	Magnitude of Casimir Force	26
4.1	Plate-Plate	26
4.2	Plate-Sphere	27
4.3	Plate-Sphere-Plate	28
4.4	Real scalar field	29
5	Conclusions	30
	Bibliography	31

Chapter 1

Introduction

En este capítulo, presentaremos los objetivos principales del trabajo. Posteriormente, dedicaremos una introducción al origen Efecto Casimir desde el punto de vista físico e histórico. Para terminar, comentaremos el origen de la energía del vacío cuántico.

1.1 Objectives and Methodology

This work is a review on the Casimir Effect. The main purpose of this work is understand the Casimir Effect theoretically and experimentally. Also, we want to see the magnitude of Casimir Effect and compare the different forces in some simple geometries.

From the theoretical point of view the key point is to relate vacuum fluctuations with forces appearing between objects. At this respect we shall introduced some mathematical tools which are relevant. In addition, we shall see how the vacuum forces where measured in the well known experiment carried out by Lamoreaux.

1.2 The origin of the Casimir Effect

The Casimir Effect is related to the Quantum Vacuum. The uncertainly principle establishes that, in a quantum system, the lower energy is different from zero. This calculus was derived for first time in 1948 by Dutch scientist H.B.G Casimir[1].

The Casimir effect has been generally taken as proof of the reality of the zero-point electromagnetic vacuum field energy.

This effect was predicted by Casimir when he was investigating with Polder the Van der Waals interaction between two atoms[2]. There was a problem with Van der Waals interaction at large distances highlighted by London's result which did not agreed with experiments. Casimir and Polder addressed the problem calculating the Van der Waals force between two atoms and the force between an atom and a perfectly conducting wall, considering the influence of retardation effects using perturbative quantum electrodynamics.

Following a suggestion by Bohr [3], Casimir studied the role of vacuum fluctuations. He found a way to derive his result by computing the shift in the electromagnetic zero-point energy due to the presence of the atoms and the walls [1].

1.2.1 Quantum Vacuum

From Classical Electrodynamics, it is known that the free electromagnetic field is described by a infinite collection of harmonic oscillators that in going to a quantum description can be properly quantized.

Therefore, we have at each point in space a quantum harmonic oscillator which have a energy different from zero in its ground state. Each mode of the electromagnetic field oscillates with a different frequency and makes a contribution of $\frac{\hbar\omega}{2}$ to the zero-point energy. So, we can view the quantum vacuum as the the combination of all zero-point fields. Summing all modes we get a divergent quantity that can be renormalized subtracting that infinity. We will show how deal with these type of infinities in next chapter.

Also, as we said before, the uncertainly principle forbids the vacuum energy of the harmonic oscillator of being zero. We can start from the Hamiltonian of the harmonic oscillator, use the uncertainly principle and minimize the energy to obtain Δx or Δp to obtaine the minimum in energy given by $\hbar\omega/2$.

The vacuum energy could be represented as virtual particles. These are particles that exist during a short time determined by the uncertainly relation $\Delta E\Delta t \geq \frac{\hbar}{2}$. Virtual particles are created as particle-antiparticle pairs that are annihilated given

an amount of energy, vacuum energy. For this reason, virtual particles are called vacuum fluctuations.

Chapter 2

Casimir Effect

En este capítulo estudiaremos el efecto Casimir en diferentes geometrías. Primero derivaremos el efecto Casimir para una configuración de unas placas plano paralelas con conductividad infinita. Teniendo cuenta de que tenemos infinitos modos de oscilación, es decir, energía infinita, aplicaremos un método para eliminarlo y obtener un resultado finito. Repetiremos el cálculo anterior considerando una de las placas con permeabilidad infinita. A continuación, hallaremos la corrección térmica al efecto Casimir en la configuración placa-placa. Posteriormente, se estudiará el efecto Casimir para la configuración placa-esfera. Usaremos este resultado para analizar el caso de que la esfera se encuentre en medio de dos placas plano paralelas. Finalmente, nos fijaremos en un campo real escalar y la aparición de fuerzas de tipo Casimir. Usaremos diferentes métodos para restar la energía infinita.

In the present chapter we are going to calculate Casimir Effect in different topologies. First we will derive the Casimir plate-plate attractive force in such configuration, then we will give an example of a Casimir repulsive force. Next we will obtain the thermal correction to the Casimir force in the plate-plate configuration. After that we will demonstrate a helpful theorem that allows us to calculate the Casimir Effect in a plate-sphere configuration. We shall use this result to obtain the Casimir's forces acting on a sphere between two parallel plates. Finally, we shall consider a scalar field theory where Casimir Effect in a Klein-Gordon field can be computed by mean of different methods to regularized the expressions and obtain a physically meaningful quantity.

2.1 Plate-Plate configuration.

2.1.1 Attractive Force

Now we are going to calculate the zero point energy of two parallel plates following the procedure described in [4].

Consider two parallel square plates of length L separated by a distance a , as shown in Figure 2.1. Moreover, the plates are such that they have infinite conductivity and uncharged. Each mode of electromagnetic field is associated with a mode of an harmonic oscillator. Hence we can write the zero-point energy as

$$H_0 = \sum_l \frac{1}{2} \hbar \Omega_l. \quad (2.1)$$

The dispersion relation for each mode is written as

$$\Omega_l = c \|\vec{k}_l\| = c(k_x^2 + k_y^2 + k_z^2)^{1/2}. \quad (2.2)$$

The wave vector k must satisfied certain boundary conditions, that in our case are such that the parallel component of the electric field is zero at the surfaces of the

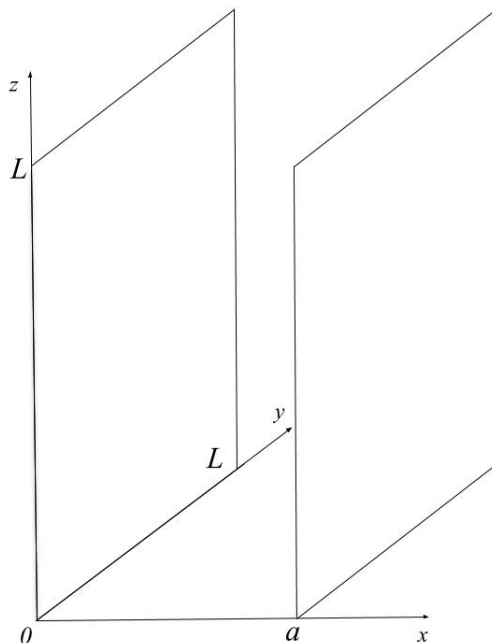


FIGURE 2.1: Parallel condenser plates.

plates. This condition implies that

$$k_x = \frac{l_x \pi}{a} \quad k_y = \frac{l_y \pi}{L} \quad k_z = \frac{l_z \pi}{L}. \quad (2.3)$$

Applying the boundary conditions to equation 2.2, we rewrite the energy for a rectangular resonator as

$$H_0^{box} = \sum_l \frac{1}{2} \hbar \Omega_l = \frac{\hbar c}{2} \sum_{pol} \sum_{l_x, l_y, l_z=0}^{\infty} \sqrt{\left(\frac{l_x \pi}{a}\right)^2 + \left(\frac{l_y \pi}{L}\right)^2 + \left(\frac{l_z \pi}{L}\right)^2}. \quad (2.4)$$

Notice that we add a sum over the polarization of the photons. We assume that the distance between the plates, a , is much smaller than the plates length, L *i.e.*

$$a \ll L \implies L \longrightarrow \infty.$$

Consequently, l_x and l_y can be considered to be continuous variables and we can use Riemann integral definition to obtain:

$$\begin{aligned} H_0^{box} &= \frac{\hbar c}{2} \sum_{pol} \sum_{l_x=0}^{\infty} \int_0^{\infty} dl_y \int_0^{\infty} dl_z \sqrt{\left(\frac{l_x \pi}{a}\right)^2 + \left(\frac{l_y \pi}{L}\right)^2 + \left(\frac{l_z \pi}{L}\right)^2} \\ &= \frac{\hbar c \pi}{2a} \sum_{pol} \sum_{l_x=0}^{\infty} \int_0^{\infty} dl_y \int_0^{\infty} dl_z \sqrt{l_x^2 + \left(\frac{l_y a}{L}\right)^2 + \left(\frac{l_z a}{L}\right)^2}. \end{aligned} \quad (2.5)$$

It is convenient to perform a change of variables $\alpha = \frac{l_y a}{L}$, $\beta = \frac{l_z a}{L}$ and use polar coordinates $\alpha = \sqrt{u} \cos(\varphi)$, $\beta = \sqrt{u} \sin(\varphi)$. The Jacobian of the transformation is denoted as $J(u, \varphi)$. It follows then

$$\begin{aligned} H_0^{box} &= \frac{\hbar c \pi L^2}{2a^3} \sum_{pol} \sum_{l_x=0}^{\infty} \frac{1}{2} \int_0^{\infty} du \int_0^{\frac{\pi}{2}} d\varphi \sqrt{l_x^2 + u} \\ &= \frac{\hbar c \pi^2 L^2}{8a^3} \sum_{pol} \sum_{l_x=0}^{\infty} \int_0^{\infty} du \sqrt{l_x^2 + u}. \end{aligned} \quad (2.6)$$

Separating the term $l_x = 0$ (that has only one direction of polarization) and summing over the polarization it follows

$$H_0^{box} = \frac{\hbar c \pi^2 L^2}{8a^3} \int_0^\infty du \sqrt{u} + 2 \sum_{l_x=1}^\infty \int_0^\infty du \sqrt{l_x^2 + u}. \quad (2.7)$$

The next step is to calculate the energy without plates, i.e, $a \rightarrow \infty$ and as we did before $L \rightarrow \infty$, then l_x, l_y and l_z are continuum variables. From 2.3 we can write:

$$H_0^{vac} = \frac{\hbar c}{2} \sum_{pol} \int_0^\infty dl_x \int_0^\infty dl_y \int_0^\infty dl_z \sqrt{\left(\frac{l_x \pi}{a}\right)^2 + \left(\frac{l_y \pi}{L}\right)^2 + \left(\frac{l_z \pi}{L}\right)^2}. \quad (2.8)$$

Following the same steps as we did above, with the same variables α, β , using polar coordinates and summing over polarizations we get

$$H_0^{vac} = \frac{\hbar c \pi^2 L^2}{8a^3} 2 \int_0^\infty dl_x \int_0^\infty du \sqrt{l_x^2 + u}. \quad (2.9)$$

The equations 2.7 and 2.9 are divergent quantities. To remove the infinity and get some physically meaningful quantity, we can calculate the difference between the two infinite energies defined by

$$\Upsilon = \frac{1}{L^2} [H_0^{box} - H_0^{vac}] = \frac{\hbar c \pi^2}{4a^3} \tilde{I}, \quad (2.10)$$

where we introduce \tilde{I} given by

$$\tilde{I} = \frac{1}{2} \int_0^\infty du \sqrt{u} + \sum_{l_x=1}^\infty \int_0^\infty du \sqrt{l_x^2 + u} - \int_0^\infty dl_x \int_0^\infty du \sqrt{l_x^2 + u}. \quad (2.11)$$

If $I(l_x) = \int_0^\infty du \sqrt{l_x^2 + u}$ we can write

$$\tilde{I} = \frac{1}{2} I(0) + \sum_{l_x=1}^\infty I(l_x) - \int_0^\infty dl_x I(l_x) = \frac{1}{2} I(0) + \sum_{l_x=0}^\infty I(l_x) - \int_0^\infty dl_x I(l_x) - I(0). \quad (2.12)$$

In order to get a finite result we use the Euler-Maclaurin formula

$$\sum_{n=0}^\infty f(n) = \int_0^\infty dx f(x) + \frac{1}{2} f(0) - \frac{1}{12} f'(0) + \frac{1}{720} f'''(0) + \dots \quad (2.13)$$

in the last equation and substituting into 2.11 to obtain

$$\tilde{I} = -\frac{1}{12}I'(l_x) + \frac{1}{720}I'''(l_x) + \dots \quad (2.14)$$

With the change $v = l^2 + u$ we can easily evaluate the derivatives and obtain: $I'(0) = 0$ and $I'''(0) = -4$, (The higher orders are 0).

We can substitute the results into equation 2.10 and write the energy per area as

$$\Upsilon(a) = -\frac{1}{720} \frac{\hbar c \pi^2}{a^3}. \quad (2.15)$$

From this last equation we can compute the force per area between the plates given by $F = -\frac{d\Upsilon}{da}$ to finally write:

$$F(a) = -\frac{1}{240} \frac{\hbar c \pi^2}{a^4}, \quad (2.16)$$

which is the result obtained by Casimir. Note that, this force is attributed to the change in the zero point energy of the vacuum in presence of the plates and without them. The Casimir effect is a quantum phenomenon (because it depends on \hbar) and relativistic (because it depends on c).

The result is an attractive force but generally depends on the geometry of the system. It could also depend on the composition of the plates.

2.1.2 Repulsive Force

The Casimir force can be repulsive if we consider the interaction between an ideal conducting plate and an infinite permeable plate[5].

So, suppose the same configuration of Figure 2.1. The boundary conditions are not 2.3, they must change due to the permeable plate. We consider that x axis possess infinite permeability and the other component is not modified.

Since the parallel component of the magnetic field B vanishes, from Faraday's Law we can see which the component $\nabla \times E$ is zero which implies that we have Neumann boundary condition:

$$k_x = \frac{\pi}{a} \left(l_x + \frac{1}{2} \right), \quad (2.17)$$

thus, the energy of the vacuum with 2.1, 2.2 and 2.17 :

$$H_0^{box} = \sum_l \frac{1}{2} \hbar \Omega_l = \frac{\hbar c}{2} \sum_{pol} \sum_{l_x, l_y, l_z=0}^{\infty} \sqrt{\frac{\pi^2}{a^2} \left(l_x + \frac{1}{2} \right)^2 + \left(\frac{l_y \pi}{L} \right)^2 + \left(\frac{l_z \pi}{L} \right)^2}. \quad (2.18)$$

Following the same procedure we used in 2.1.1 and evaluating the difference of two infinite energies, we obtain a finite repulsive force

$$F(a) = \frac{7\hbar c \pi^2}{1920a^4}. \quad (2.19)$$

Another way, if Dirichlet boundary conditions are chosen on the plane $x = 0$ and Neumann conditions on the plane $x = a$, i.e, mixed boundary conditions [6], we get the announced repulsive force.

2.1.3 Temperature correction.

In real situations the systems will be at finite temperature, so it is pertinent to estimate the corrections that finite temperature effects may have in Casimir's forces. In this section we are going to calculate thermal effects in a system composed by two parallel plates following the derivation presented in [7].

At low temperatures the corrections to the original Casimir result due to nonzero temperature are negligibly small. On the contrary, if the temperature is high enough the temperature corrections becomes important. This behaviour is usually called "the classical limit" because it is determined by thermal photons.

The grand canonical partition function for an ideal Bose gas writes:

$$\mathcal{L}(T, V, \mu) = \prod_k \frac{1}{1 - z e^{-\beta E_k}}. \quad (2.20)$$

For a photon gas we have that $E_k = \hbar \omega_k$ is the energy of each photon with wave vector k . We fix the fugacity z to $z = 1$

The energy is obtained from the partition function as $E = -\partial_\beta \log \mathcal{L}$. This yields

$$E = \sum_k \sum_{pol} \frac{\hbar \omega_k}{e^{\beta \hbar \omega_k} - 1}. \quad (2.21)$$

We know that $\omega = c\|\vec{k}\|$ and from equation 2.3 we can write the energy as:

$$E = \sum_{n_x, n_y, n_z=0}^{\infty} \sum_{pol} \frac{\hbar c \sqrt{\left(\frac{n_x \pi}{a}\right)^2 + \left(\frac{n_y \pi}{L}\right)^2 + \left(\frac{n_z \pi}{L}\right)^2}}{e^{\beta \hbar c \sqrt{\left(\frac{n_x \pi}{a}\right)^2 + \left(\frac{n_y \pi}{L}\right)^2 + \left(\frac{n_z \pi}{L}\right)^2}} - 1}. \quad (2.22)$$

Following the same lines than those taken to reach 2.1.1, we use the definition of Riemann Integral and change to polar coordinates to obtain

$$E = \frac{\hbar c \pi^2 L^2}{4a^3} \sum_{n_x=0}^{\infty} \sum_{pol} \int_0^{\infty} dr \frac{\sqrt{(n_x)^2 + r}}{e^{\frac{\beta \hbar c \pi}{a} \sqrt{(n_x)^2 + r}} - 1}. \quad (2.23)$$

Implementing the change of variables $u = \sqrt{n_x^2 + r}$ and $u = v + n_x$ it follows

$$\begin{aligned} \frac{E}{L^2} &= \frac{\pi^2 \hbar c}{2a^3} \sum_{n_x=0}^{\infty} \sum_{pol} \int_0^{\infty} \frac{(v + n_x)^2}{e^{\frac{\beta \hbar c \pi}{a} (n_x + v)} - 1} dv \\ &= \frac{\hbar c \pi^2}{2a^3} \sum_{n_x=0}^{\infty} \sum_{pol} \frac{-n_x^2 \log\left(1 - e^{-\frac{\beta \hbar c \pi n_x}{a}}\right)}{\beta \hbar c \pi / a} + \frac{2n_x Li_2\left(e^{-\frac{\beta \hbar c \pi n_x}{a}}\right)}{(\beta \hbar c \pi / a)^2} + \frac{2Li_3\left(e^{-\frac{\beta \hbar c \pi n_x}{a}}\right)}{(\beta \hbar c \pi / a)^3}. \end{aligned} \quad (2.24)$$

The first term is the most important one as the others are exponentially small. Introducing the definition $\alpha = \frac{\beta \hbar c \pi}{a}$ we can write

$$\frac{E}{L^2} = -\frac{\pi}{2\beta a^2} \sum_{n_x} n_x^2 \log(1 - e^{-\alpha n_x}). \quad (2.25)$$

To analyze this expression we will use the Poisson summation formula:

$$\sum_{n=-\infty}^{\infty} f(n) = 2\pi \sum_{n=-\infty}^{\infty} a(2\pi n), \quad (2.26)$$

where $a(\mu) = \frac{1}{2\pi} \int_{-\infty}^{\infty} dx f(x) e^{i\mu x}$.

If we consider $f(n) = n^2 \log(1 - e^{-\alpha|n|})$ the the Poisson formula leads to:

$$\sum_{n=-\infty}^{\infty} f(n) = f(0) + 2 \sum_{n=1}^{\infty} n^2 \log(1 - e^{-\alpha n}), \quad (2.27)$$

notice that $f(n) = f(-n)$. We can do the same with the right-hand side of 2.26 because $a(-\mu) = a(\mu)$ to get

$$\begin{aligned} \sum_{n=-\infty}^{\infty} f(n) &= \sum_{k=-\infty}^{\infty} a(2\pi n) \\ &= 2\pi a(0) + 4\pi \sum_{n=1}^{\infty} a(2\pi n), \end{aligned} \quad (2.28)$$

with $f(0) = 0$. Hence the energy per unit area is given by

$$\frac{E}{L^2} = -\frac{\pi}{2\beta a^2} \sum_{n=1}^{\infty} n^2 \log(1 - e^{-\alpha n}) = -\frac{\pi}{2\beta a^2} \left(\pi a(0) + 2\pi \sum_{n=1}^{\infty} a(2\pi n) \right), \quad (2.29)$$

since $f(x)$ is an even function we can calculate the coefficient $a(\mu)$ as

$$a(\mu) = \frac{1}{\pi} \int_0^{\infty} dx f(x) \cos(\mu x) = -\frac{1}{\pi} \int_0^{\infty} dx x^2 \log(1 - e^{-\alpha x}) \cos(\mu x). \quad (2.30)$$

Alternatively we can consider the expression

$$-\frac{1}{\pi} \partial_{\mu}^2 \int_0^{\infty} dx \log(1 - e^{-\alpha x}) \cos(\mu x) = -\frac{1}{\pi} \partial_{\mu}^2 \left\{ \frac{\alpha - \pi \mu \coth(\frac{\pi \mu}{\alpha})}{2\mu^2} \right\} \quad (2.31)$$

as a function of β . Because $\alpha = \frac{\beta \hbar c \pi}{a}$, and $\beta = \frac{1}{k_b T}$, we take the high temperature limit as $\alpha \ll 1$ and write $\coth(x)$ when $x \gg 1$ as $\coth(x) \simeq 1 + 2e^{-2x}$.

If we apply the above considerations on eq. 2.31 it follows that

$$-\partial_{\mu}^2 \left\{ \frac{\alpha - \pi \mu (1 + 2e^{-\frac{\pi \mu}{\alpha}})}{2\pi \mu^2} \right\} = -\frac{1}{\mu^3} + \frac{3\alpha}{\pi \mu^4} + \dots \quad (2.32)$$

The last terms are exponentially small, so we will neglect them and proceed to obtain the solution for the coefficients $a(\mu)$. For $a(0)$ from 2.31 we obtain $a(0) = -\frac{\pi^3}{45\alpha^3}$.

Then, from 2.29

$$\frac{E}{L^2} = \frac{\pi}{2\beta a^2} \left\{ \frac{-\pi^4}{45\alpha^3} + \sum_{\mu=1}^{\infty} -\frac{2\pi}{\mu^3} + \frac{6\alpha}{\mu^4} + \dots \right\}. \quad (2.33)$$

We detract the first term which correspond with the self energy ans knowing that $\mu = 2\pi n$ then

$$\frac{E}{L^2} = \frac{\pi}{2\beta a^2} 2\pi \sum_{n=1}^{\infty} -\frac{1}{(2\pi n^3)} + \dots \quad (2.34)$$

In this last expression we recognize the Zeta Riemann function $\zeta(3)$ in terms of which the energy per unit area is

$$\frac{E}{L^2} = -\frac{k_B T \zeta(3)}{8\pi a^2}. \quad (2.35)$$

Consequently, the force per unit area will be $F = -\frac{dE}{da}$ given by

$$F = -\frac{k_B T \zeta(3)}{4\pi a^3}. \quad (2.36)$$

That is the dominant term of the Casimir force for the case studied.

2.2 Plate-Sphere configuration

In this section we are going to introduce the Proximity Force Theorem [8] which allows the computation of proximity forces between curved objects. The theorem states that:

The force between two curved objects in close proximity is proportional to the interaction potential per unit area between two flat surfaces made of the same material

We shall present a sketch of the proof goes as follows, consider the proximity energy associated with a curved gap of variable width D :

$$V_p = \iint e(D) d\sigma, \quad (2.37)$$

where $e(D)$ is in the interaction energy per unit area of two parallel surfaces at separation D and σ is the area of the gap. We neglect further corrections to the proximity energy.

We define Γ as the mean gap surface and $D(u, v) = n_R - n_L$. We say that n_R and n_L are the normal displacements. So, we have the gap located on the right-hand

and left-hand sides. $D(u, v)$ is the distance between the two sides Γ_R, Γ_L of the gap.

Then, the gap width is a function of the position on the surface, Γ . This is specified by two coordinates u and v .

We can see that $e(D)$ is a function of one variable, then we must convert the surface integral into a 1D integral. Therefore, we have to consider a family of curves built on the surface corresponding to constant values of D . In such situation we can write the proximity energy as

$$V_p = \int e(D)J(D)dD, \quad (2.38)$$

where $J(D)$ is the characteristic of the geometry of the gap. Now, we introduce α which specifies the geometry of the gap and β which specifies the structure of the surface region. After that, we can rewrite, the proximity energy in general case:

$$V_p = \int \int e(\beta, D)J(\alpha, D)dD. \quad (2.39)$$

Finally, we are going to apply this theorem in case that we have a gap with variable parabolic width(that correspond with the plate-sphere case).

We set the mean gap gently curved. So, u, v on the surface may be taken as cartesian x, y coordinates and the normal coordinate n used to specify the gap may be taken as the cartesian coordinate z . So, $D = Z_R - Z_L$.

We consider that we have a gap D which has a least value $D(x, y) = S$ at $x = y = 0$. The Taylor expansion of $D(x, y)$ is:

$$D(x, y) = s + \frac{1}{2}D_{xx}x^2 + \frac{1}{2}D_{yy}y^2. \quad (2.40)$$

The derivatives can be written in terms of the principal radii of curvature R_x, R_y of the surface obtained by plotting the gap width D as a function of x, y .

Next, implementing the change of variables: $\xi = \frac{x}{\sqrt{2R_x}}$ and $\eta = \frac{y}{\sqrt{2R_y}}$, which implies that $D = s + p^2$ and $p^2 = \xi^2 + \eta^2$.

It follows that

$$\begin{aligned} V_p(s) &= \iint dx dy e(D) = \sqrt{2R_x R_y} \iint d\xi d\eta e(D) \\ &= \sqrt{2R_x R_y} \int_0^\infty dp 2\pi p e(D) = \sqrt{2R_x R_y} \int_{D=s}^\infty dD e(D). \end{aligned} \quad (2.41)$$

Defining $\sqrt{2R_x R_y}$ as \bar{R} which is the geometric mean of the two principal radii of curvature. We finally get

$$V_p(s) = 2\pi \bar{R} e(s). \quad (2.42)$$

We can write the force using the negative of the partial derivative of $V_p(s)$ with respect to s to conclude that the proximity force F is given by

$$F(s) = 2\pi \bar{R} e(s). \quad (2.43)$$

From equations 2.15 and 2.43 it is possible to obtain the Casimir force for the configuration shown in the figure 2.2. In such configuration we have an sphere with radius R and a plate with length L in close proximity. The separation between the surfaces is denoted by a and the force is given by.

$$F(a) = 2\pi R \frac{\hbar c \pi^2}{720 a^3}. \quad (2.44)$$

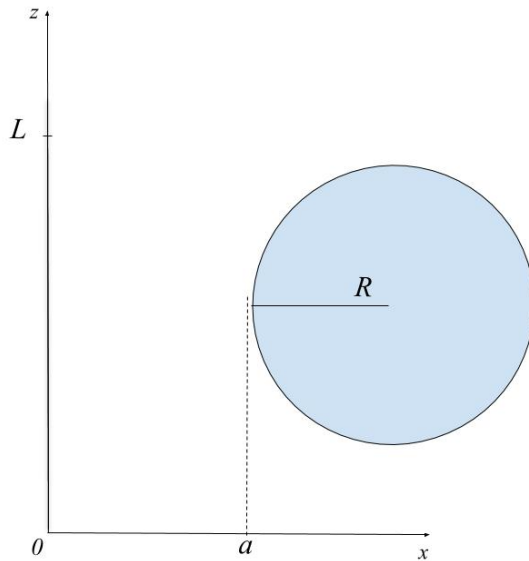


FIGURE 2.2: Plate-Sphere configuration.

2.3 Plate-Sphere-Plate configuration

In this configuration, the sphere is between two plates separated a distance a as we shown in Figure 2.3. The plates have the same length, L and the sphere has a radius R . The displacement of the sphere to plate 1 or 2 is defined by x .

The net force can be represented as $F_{net} = F_1 + F_2$. Where F_1 and F_2 are given by eqn. 2.43, and have different direction, i.e, in which F_1 is repulsive, F_2 becomes attractive, because when the system is in equilibrium ($x = 0$) the net force must be zero. We are going to calculate the Casimir Energy when the system is not in equilibrium. Assuming that F_1 is repulsive and F_2 attractive.

$$F_1(a) = \frac{\alpha R}{\left(\frac{a}{2} + x\right)^3}. \quad (2.45)$$

$$F_2(a) = -\frac{\alpha R}{\left(\frac{a}{2} - x\right)^3}. \quad (2.46)$$

with $\alpha = \frac{2\pi\hbar c\pi^2}{720}$.

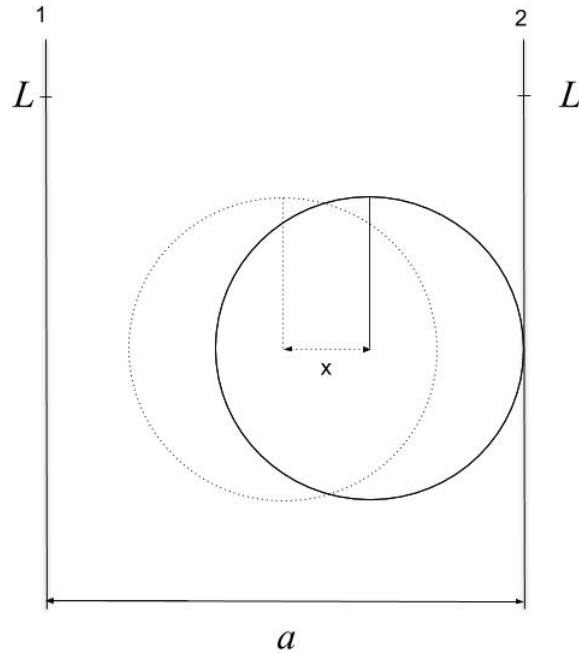


FIGURE 2.3: Plate-Sphere-Plate configuration.

The net force is $F_{net} = F_1 + F_2$, after some manipulations one can obtain

$$F_{net} = -32\alpha x R \frac{3a^2 + 4x^2}{(a^2 - 4x^2)^3}. \quad (2.47)$$

In the limit: $x \ll a$ the force is given by

$$F_{net} = -94\alpha R \frac{x}{a^4} \quad (2.48)$$

2.4 Scalar Field Theory

We shall show very briefly in this section how Casimir forces emerge in the context of scalar field theories.

2.4.1 A brief introduction of Quantum Field Theory

Quantum Field Theory combines Quantum Mechanics and Special Relativity, *i.e.* is a Lorentz covariant theory which allows to study systems for which both Quantum and Relativistic effects are important.[9]

We shall start from Poincaré covariant free classical fields. To quantize these fields, a method known as canonical quantization can be used. The Canonical Quantization consists of promoting the classic coordinates and momenta to quantum mechanical operators that should satisfy the commutation relations. The coordinates $q(t)$ and momenta $p(t)$ are replaced by the fields $\varphi(\mathbf{x}, t)$ and $\Pi_\varphi(\mathbf{x}, t)$ respectively.

The fields can be expanded in terms of plane waves (Fourier series). The coefficients are promoted to operators corresponding to the creation and annihilation operators of a quantum harmonic oscillator. Vacuum excitations produced by the field operators are particles and antiparticles. So, particles are described by the fields that are operators on the quantum mechanical Hilbert space of the particles states.

Consider a real scalar field $\varphi(x)$ which describes spin-0 bosons in two dimensional space-time and is invariant under Lorentz transformations. The Lagrangian density for this field is

$$\mathcal{L} = \frac{\hbar^2}{2}(\partial_\mu\varphi)(\partial^\mu\varphi) - \frac{1}{2}m^2c^2\varphi^2. \quad (2.49)$$

The equations of motion for each is given by the Euler-Lagrange equations. Introducing the Lagrangian we can get the Klein-Gordon equation[10]

$$\square_2\varphi(t, x) + \frac{m^2c^2}{\hbar^2}\varphi(t, x) = 0, \quad (2.50)$$

where $\square_2 = \frac{1}{c^2}\frac{\partial^2}{\partial t^2} - \frac{\partial^2}{\partial x^2} = \partial_\mu\partial^\mu$. Alternatively it is possible to derived Klein-Gordon equation starting from the relativistic energy for free particles

$$E = \sqrt{p^2c^2 + m^2c^4}, \quad (2.51)$$

and making the replacement $E \rightarrow i\hbar\partial_t$ and $p \rightarrow -i\hbar\nabla$.

In the next section we will calculate Casimir effect in a scalar field. The derivation closely follows [6].

2.4.2 Local description of Casimir effect

We start form the vacuum energy densities to determine the total energy of the ground state of the field. The total energy of the vacuum will be obtained by the integration of the energy density over the quantization volume. The energy density can be obtained from the expectation value of the energy density operator of the quantized field in the vacuum state.

First we need to apply Noether's Theorem to compute the energy-momentum tensor [11]. The energy-momentum tensor is written as

$$T^\mu{}_\nu = \frac{\partial\mathcal{L}}{\partial(\partial_\mu\varphi)}\partial_\nu\varphi - \delta^\mu_\nu\mathcal{L}, \quad (2.52)$$

where \mathcal{L} is the Lagrangian density of the real scalar field defined in 2.49.

In particular we can write the energy density operator of the scalar field T_{00} .

$$T_{00} = \frac{\hbar c}{2} \left\{ \frac{1}{c^2} [\partial_t\varphi(t, x)]^2 + [\partial_x\varphi(t, x)]^2 + \frac{m^2c^2}{\hbar^2} [\varphi(t, x)]^2 \right\}. \quad (2.53)$$

To calculate the energy densities. First, we are going to calculate the density energy of a real scalar field with on an interval $0 \leq x \leq a$ with Dirichlet boundary conditions: $\varphi(t, 0) = \varphi(t, a) = 0$. After that, we will calculate the energy of free Minkowski space. That allow us, as we did in the previous section, to obtain a physical result as a subtraction of the two energy densities.

The positive and negative solutions of Klein-Gordon equation, that satisfy the boundary conditions, are

$$\varphi_n^{(\pm)} = \sqrt{\frac{c}{a\omega_n}} e^{\mp i\omega_n t} \sin k_n x. \quad (2.54)$$

If we quantized the real scalar field in the interval where they are defined, it follows

$$\varphi(t, x) = \sum_n (a_n \varphi_n^{(+)}(t, x) + a_n^+ \varphi_n^{(-)}), \quad (2.55)$$

where a_n and a_n^+ are the annihilation and creation operators respectively which fulfill the commutation relations $[a_n, a_{n'}^+] = \delta_{nn'}$ and $[a_n, a_{n'}] = [a_n^+, a_{n'}^+] = 0$.

The vacuum state, where there is not particles, is defined as

$$a_n |0\rangle = 0. \quad (2.56)$$

Hence, we can calculate the expectation value of the energy density operator in the vacuum state using 2.53, 2.55 and the commutation relations

$$\langle 0 | T_{00}(t, x) | 0 \rangle = \frac{\hbar}{2a} \sum_{n=1}^{\infty} \omega_n - \frac{m^2 c^4}{2a\hbar} \sum_{n=1}^{\infty} \frac{\cos 2k_n x}{\omega_n}. \quad (2.57)$$

At last, if we integrate over all the interval which lead us the density energy of the field

$$E_0(a, m) = \int_0^a \langle 0 | T_{00}(t, x) | 0 \rangle dx = \frac{\hbar}{2} \sum_{n=1}^{\infty} \omega_n. \quad (2.58)$$

Note that the oscillating term in eqn 2.57 does not affect to the total energy.

We will repeat the computations for a scalar field define in the entire real axis $-\infty < x < \infty$.

The positive and negative solutions of Klein-Gordon equations are in this case

$$\varphi_k^{(\pm)} = \sqrt{\frac{c}{4\pi\omega_n}} e^{\mp i(w_n t - kx)}. \quad (2.59)$$

We can write the field operator as

$$\varphi(t, x) = \int_{-\infty}^{\infty} dk \left(a_k \varphi_k^{(+)}(t, x) + a_k^+ \varphi_k^{(-)} \right), \quad (2.60)$$

and must follow similar commutation relations $[a_k, a_{k'}^+] = \delta(k - k')$ and $[a_k, a_{k'}] = [a_k^+, a_{k'}^+] = 0$.

The vacuum state of the Minkowski space is

$$a_k |0_M\rangle = 0. \quad (2.61)$$

Therefore, the fluctuation of the operator in the vacuum state, is obtained with [2.53](#), [2.60](#) and commuting relations:

$$\langle 0 | T_{00}(t, x) | 0 \rangle = \frac{\hbar}{4\pi} \int_{-\infty}^{\infty} dk \omega_k. \quad (2.62)$$

Finally, the energy density of the Minkowski is space can be determined integrating over all Minkowski space, whose length is denoted by L .

$$E_{0M} = \langle 0 | T_{00}(t, x) | 0 \rangle L = \frac{\hbar}{2} \int_{-\infty}^{\infty} \frac{dk}{2\pi} \omega_k L. \quad (2.63)$$

We have obtained two energies that diverge, now we need to regularize the results obtain a Casimir Force. In the next section we use two techniques to deal with such regularization.

2.4.3 Casimir effect with cutoff regularization

From eqn. [2.58](#) we have the zero point energy of real scalar field of an interval. The frequency is obtained from the relativistic energy from free particles [2.51](#) dividing by \hbar .

$$\omega_n = \left(\frac{m^2 c^4}{\hbar^2} + c^2 k_n^2 \right)^{1/2}, \quad (2.64)$$

where k_n is a discrete variable defined by $k_n = \frac{\pi n}{a}$. That give us

$$E_0(a, m) = \frac{\hbar}{2} \sum_{n=1}^{\infty} \omega_n = \frac{\hbar}{2} \sum_{n=1}^{\infty} \left(\frac{m^2 c^4}{\hbar^2} + \frac{c^2 \pi^2 n^2}{a^2} \right)^{1/2}. \quad (2.65)$$

For the case of free Minkowski space, k is a continuum variable, so the in the frequency should be an integral over the variable. From eqn. 2.63 the total energy of the Minkowski space:

$$E_{0M}(m) = \frac{\hbar}{2} \int_{-\infty}^{\infty} \frac{dk}{2\pi} w_k L = \frac{\hbar}{2\pi} \int_0^{\infty} dk \left(\frac{m^2 c^4}{\hbar^2} + c^2 k^2 \right)^{1/2} L. \quad (2.66)$$

The energies of the vacuum, E_0 and E_{0M} , are divergent. So, to subtract the infinite energy of the vacuum we need to use a regularization procedure. For such purpose, let us introduced some exponential cutoff functions that converge faster than the terms that diverge. These functions converge when a parameter δ goes to zero. It is convenient to introduce such regularization inside the summations.

We will consider, for simplicity, a massless field with $m = 0$ in 2.65 and introduce the cutoff function $\exp(-\delta c k_n)$, we can rewrite the vacuum energy as

$$E_0^{(\delta)}(a) = \frac{\hbar}{2} \sum_{n=1}^{\infty} \frac{c\pi n}{a} \exp(-\delta c\pi n/a), \quad (2.67)$$

and taking account that $\sum_{n=1}^{\infty} n \exp(-\delta c\pi n/a) = \frac{1}{4} \sinh^{-2}(\delta c\pi/2a)$. Then

$$E_0^{(\delta)}(a) = \frac{\hbar c\pi}{8a} \sinh^{-2}(\delta c\pi/2a). \quad (2.68)$$

If δ goes to zero we can perform an expansion of $\sinh^{-2}(x)$ that gives leads to

$$E_0^{(\delta)}(a) = \frac{\hbar a}{2\pi c\delta^2} - \frac{\hbar c\pi}{24a} + \mathcal{O}(\delta^2). \quad (2.69)$$

We follow the same procedure for the total energy of Minkowski space, applying the cutoff regularization and keeping the case of massless field, it follows

$$E_{0M}^{(\delta)} = \frac{\hbar c}{2\pi} \int_0^{\infty} dk k \exp(-\delta c k) L = \frac{\hbar L}{2\pi c\delta^2}. \quad (2.70)$$

If we separate out the interval $(0, a)$ of entire axis. This can be written as

$$E_{0M}^{(\delta)}(a) = \frac{E_{0M}^{(\delta)}}{L}a = \frac{\hbar a}{2\pi c\delta^2}. \quad (2.71)$$

Finally, we calculate the finite energy of the vacuum, as we know, the difference between the infinite energies and gives us a finite result, which gives:

$$E^{(\delta)}(a) = E_0^{(\delta)}(a) - E_{0M}^{(\delta)}(a) = -\frac{\hbar c\pi}{24a} + \mathcal{O}(\delta^2). \quad (2.72)$$

In the limit $\delta \rightarrow 0$, the Casimir energy for a scalar field is:

$$E = -\frac{\hbar c\pi}{24a}, \quad (2.73)$$

and, again the force is $F = -\frac{dE}{da}$, then we conclude that the the Casimir force is

$$F = -\frac{\hbar c\pi}{24a^2}. \quad (2.74)$$

2.4.4 Casimir effect with Abel-Plana formula

An alternative way to regularized the relevant quantities is use a summation formula known as Abel-Plana formula [6] which reads

$$\sum_{n=0}^{\infty} F(n) - \int_0^{\infty} F(t)dt = \frac{1}{2}F(0) + i \int_0^{\infty} \frac{dt}{e^{2\pi t} - 1} (F(it) - F(-it)). \quad (2.75)$$

We will repeat the methods of last section, to study the Casimir Effect in a scalar field but using the Abel-Plana formula instead of cutoff functions.

First we start from the energy of the vacuum in an interval scalar field. We take $\sum_{n=1}^{\infty} F(n)$ as 2.65. And separating the term with $n = 0$ such that:

$$\sum_{n=0}^{\infty} F(n) = \frac{mc^2}{2} + \frac{\hbar}{2} \sum_{n=1}^{\infty} \left(\frac{m^2 c^4}{\hbar^2} + \frac{c^2 \pi^2 n^2}{a^2} \right)^{1/2} = \frac{mc^2}{2} + E_0(a, m). \quad (2.76)$$

From eqn 2.66, taking account the change of variable $ak = \pi t$ we have

$$\int_0^{\infty} dt F(t)dt = \frac{E_{0M}(m)a}{L} = E_{0M}(a, m). \quad (2.77)$$

We compute the difference between 2.76 and 2.77 to write

$$E(a, m) = E_0(a, m) - E_{0M}(a, m) = \sum_{n=1}^{\infty} F(n) - \int_0^{\infty} dt F(t) dt \quad (2.78)$$

If we apply Abel-Plana formula it follows

$$E(a, m) = -\frac{mc^2}{4} + i\frac{\pi\hbar c}{2a} \int_0^{\infty} \frac{dt}{e^{2\pi t} - 1} (G_A(it) - G_A(-it)), \quad (2.79)$$

expression we need to check in order to see if it is not divergent.

If we define the right hand part as

$$G_A(t) \equiv (A^2 + t^2)^{1/2}, \text{ with } A = \frac{mca}{\pi\hbar}, \quad (2.80)$$

it is easy to prove that

$$G_A(it) - G_A(-it) = 2i(t^2 - A^2)^{1/2}\theta(t - A). \quad (2.81)$$

When we substitute the previous result into eqn. 2.79, this integral can be solved to get

$$E(a, m) = -\frac{mc^2}{4} - \frac{\hbar c}{4\pi a} \int_{2\mu}^{\infty} \frac{\sqrt{y^2 - 4\mu^2}}{e^y - 1} \quad (2.82)$$

with $\pi A = mca \hbar = \mu$.

Again, for simplicity, we consider a massless field ($\mu = 0$), in such case

$$E(a) = -\frac{\hbar c}{4\pi a} \int_0^{\infty} \frac{y dy}{e^y - 1} = -\frac{\hbar c \pi}{24a}, \quad (2.83)$$

which is the result expressed in eqn. 2.73.

Chapter 3

Experimental demonstration

En este capítulo, se dará una explicación de como se ha medido el efecto Casimir. Para ello, nos basaremos en el primer experimento en el que se midió con menor error. Fue hecho por Lamoreaux en 1996 y empleó un péndulo de torsión. Debido a la dificultad de usar placa plano paralelas, usó en su lugar una placa y una esfera [12].

The measurement of the Casimir force is a complex task. Given the small value of the force for the experimentally accessible surface areas, the force sensitivity of the available measurement techniques has been a severe limitation. Another limitation is that the separation distances where the Casimir force becomes measurable are very small and their accurate determination has been difficult. Given that the force has a very strong dependence on the separation and on the geometrical and material properties of the boundary surfaces, the comparison between experiment and theory is a challenging task.

Lamoreaux did in 1996 the first successfully demonstration of the Casimir force [12]. In his experiment he used the plate-sphere configuration. The Casimir Effect for this configuration is given by:

$$F_c(a) = 2\pi R \frac{\hbar c \pi^2}{720 a^3}. \quad (3.1)$$

This equation needs some corrections in order to compare with the experiment:

1. The effect of temperature ($T = 300^\circ K$). Temperature corrections were computed by Brown and Maclay [13]. They calculate the correction temperature in the energy density (T^{00}) of plate-plate configuration using the canonical ensemble average. Then, one compute the surface area as $E = aT^{00}$. Finally, using proximity force theorem for plate-sphere configuration. It follows

$$F_c^T(a) = F_c(a) \left(1 + \frac{720}{\pi^2} f(x) \right). \quad (3.2)$$

We define $x = k_B T a / \hbar c$ and $f(x)$ as:

$$f(x) = \begin{cases} (x^3/2\pi)\zeta(3) - (x^4\pi^2/45) & \text{if } x \leq 1/2 \\ (x/8\pi)\zeta(3) - (\pi^2/720) & \text{if } x > 1/2. \end{cases} \quad (3.3)$$

2. Another important correction is related to the fact that conductivity is not infinite. For finite conductivity Sweinger et al. [14] demonstrate that

$$F_c(a) = \left(1 + \frac{4c}{a\omega_p} \right), \quad (3.4)$$

ω_p represent the plasma frequency for the conductor.

Back to the experiment of Lamoreaux, he used a system based in a torsion pendulum in a vacuum chamber. A vacuum of order $10^{-4} torr$. A feedback system was used to keep the torsion pendulum angle fixed (two compensator plates form a capacitor with respect to the pendulum body). A DC voltage was applied to the compensators to keep the torsion pendulum angle fixed. Also a voltage of $7.5V$ was applied to the compensators in order to linearize the effect of the small correction voltage δV . Its important to mention that was used a solenoid activated pungler to press the plates gently together during the alignment. Thus, the plates could be brought much closer. The flat plate had a $2.54cm$ of diameter, it was placed on the arm of torsion pendulum. The sphere with radius of $11.3cm$, it was mounted micropositioning assembly.

Lamoreaux measured the Casimir Force by stepping the voltage applied to the piezoelectric stack translators. For each step, he measured the restoring force.

This must cause change in δV to compensate the change in the angle of the torsion pendulum. This voltages counteracting were a measure of Casimir force. The experiment gave 32 values a_i for the relative plate position.

The system calibration was obtained through electrical measurements based on the variations of the capacitance between the plates as a function of separation. With the plates separated but externally shorted together, there was an apparent large potential, this potential was easily canceled by setting an applied voltage between the plates to give a minimum δV .

The piezoelectric stack translators give very accurate and reproducible relative changes in the plate separation; the absolute separation was determined by measuring the residual electrical attraction between the plates as a function of separation.

When the electric force is subtracted the measured residual force it follows that

$$F_c^m = F(a_i) - \frac{\beta}{a_i} - b, \quad (3.5)$$

where a_0 is a fit parameter which gives the absolute plate separation, b and β are constants to be determined.

The magnitude of Casimir force was determined by using linear least squares to determine a parameter δ for each sweep such that:

$$F_c^m = (1 + \delta)F(a_i^T) + b'. \quad (3.6)$$

The most important result was given with accuracy of order 5%.

Chapter 4

Magnitude of Casimir Force

En este capítulo, se analizarán los resultados obtenidos. Para ello se representarán gráficamente las fuerzas calculadas. Usaremos que la distancia entre la superficies (o del campo escalar) sean entre $0.5 - 8\mu\text{m}$.

4.1 Plate-Plate

The next figure represent the eqn. 2.16 and 2.36. We present the results in logarithmic scale and absolute value.

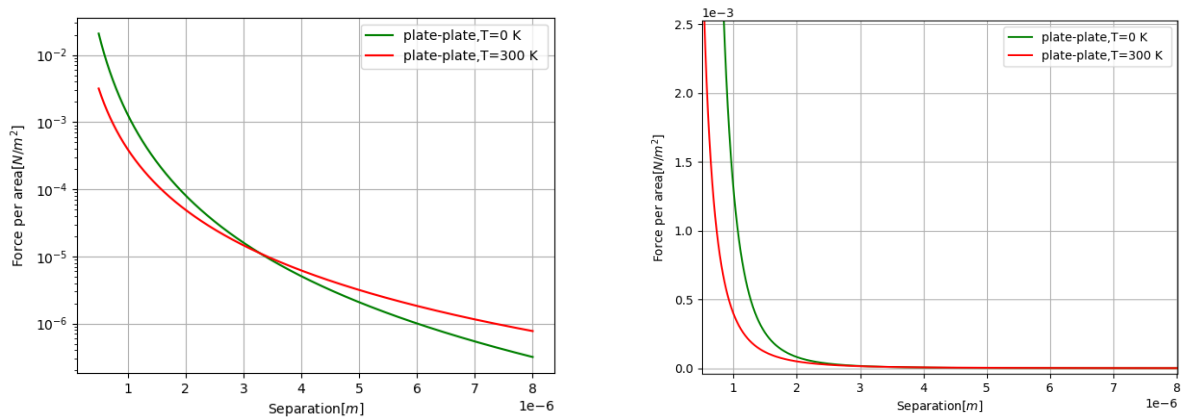


FIGURE 4.1: Plate-Plate configuration for $T = 0^\circ\text{K}$ eqn. 2.16 and for $T = 300^\circ\text{K}$ eqn. 2.36.

The thermal correction has a lower value to the force for short separation. At one point both force are the same. So, we can reproduce the plate-plate without temperature using the thermal correction.

A comparison between 2.16 and 2.19 which correspond to the attractive and repulsive force respectively. We can see that the repulsive force has a similar magnitude with attractive force.

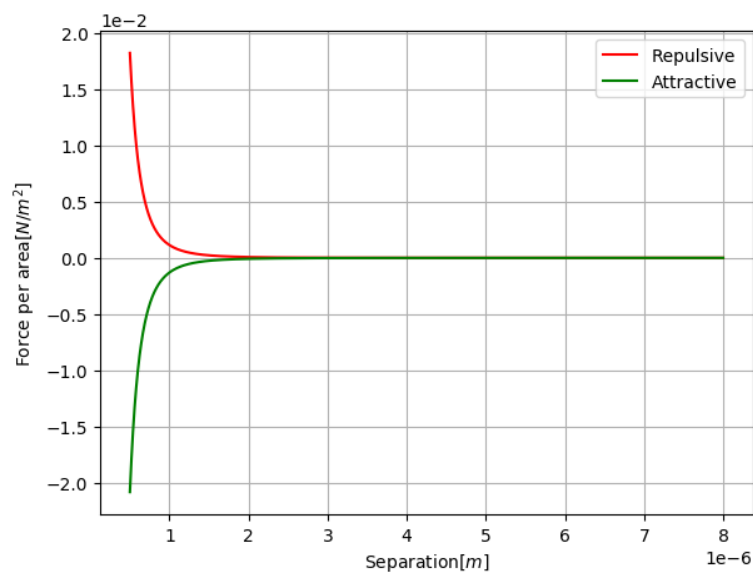


FIGURE 4.2: Attractive force eqn. 2.16 and repulsive force eqn 2.19.

4.2 Plate-Sphere

We consider that the radius of the sphere is $0.116m$. Now we compare eqn. 2.44 and 3.2. We see that the effect of the temperature in the Casimir force is only correction that shift the value of the force. We note that the thermal correction has the same magnitude in short distances.

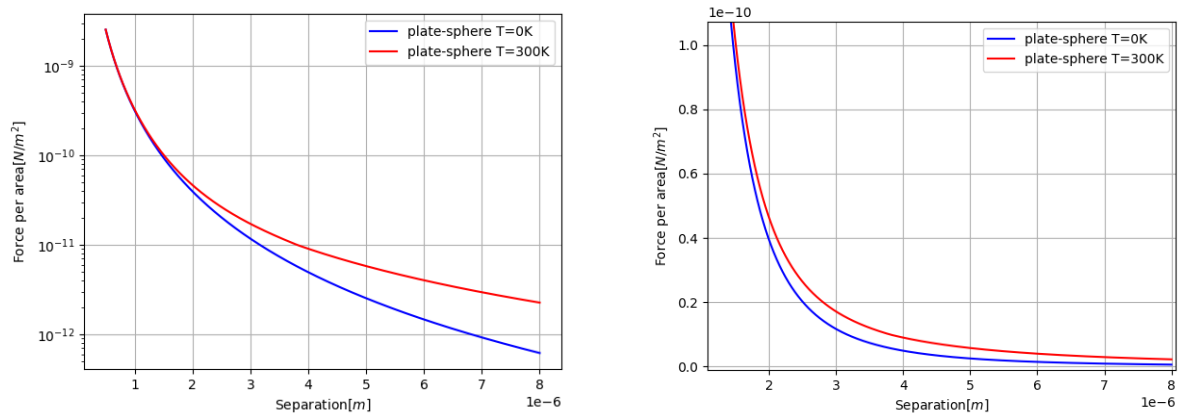


FIGURE 4.3: Plate-Sphere configuration for $T = 0^\circ K$ eqn. 2.44 and for $T = 300^\circ K$ eqn. 3.2.

4.3 Plate-Sphere-Plate

The next figure represent eqn. 2.48. We consider a small separation of the equilibrium $x = 10^{-9}m$. The magnitude of this force depend of the distance that separate of the equilibrium. This force has the same magnitude that the plate-sphere configuration as we expected. In this case the force goes to zero more fast than the other cases.

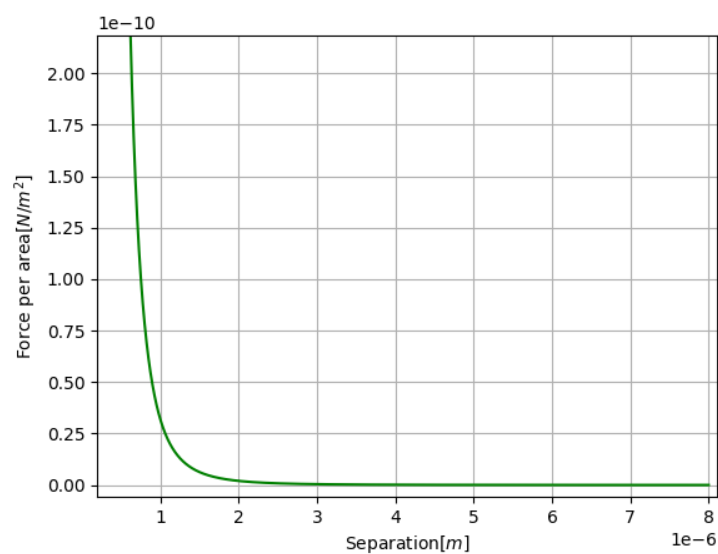


FIGURE 4.4: Plate-Sphere-Plate configuration for small displacement of the sphere, eqn. 2.48.

4.4 Real scalar field

The last figure corresponds to eqn. 2.74. That force is especially small in all distances.

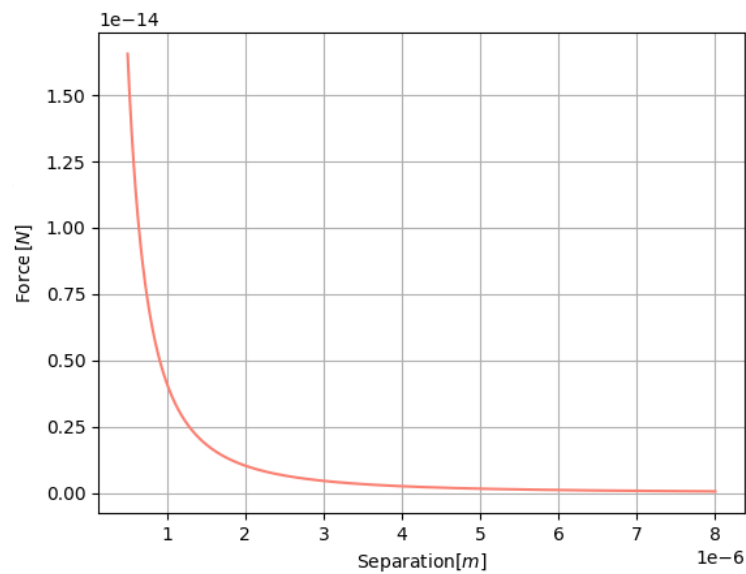


FIGURE 4.5: Casimir force of the real scalar field, eqn. 2.74

As we see to measure a Casimir force we need to put the surfaces too close. That is one of the reasons that measuring a Casimir force is a difficult task.

Chapter 5

Conclusions

In this work we have studied the basic concepts of Casimir Effect. The summary of our study is as follows:

- We have learned how vacuum energy fluctuations lead to forces, namely Casimir Effect.
- We have analytically computed Casimir forces in different configurations. Besides, we have studied a thermal correction in the case of high temperatures.
- We have learned how to work with divergent quantities using new mathematical tools we have not used in our undergraduate courses. Such as Euler-Maclaurin formula, cutoff functions and Abel Plana formula. Obtaining meaningful physical results.
- We have acquired a basic knowledge of Quantum Field Theory. We have made a canonical quantization of real scalar field.
- We have studied an experiment where Casimir Effect have been measured.
- Finally we have shown the different magnitude of the Casimir forces for different configurations and body surfaces.

A continuation of this work would be the study of Casimir Effect using Quantum Electrodynamics. Also, we could study the Casimir Effect in a topologically nontrivial curved space.

Bibliography

- [1] H. B. G. Casimir. On the attraction between two perfectly conducting plates. *Proc. K. Ned. Akad. Wet.*, 51:793–795, 1948.
- [2] H. B. G. Casimir and D. Polder. The influence of retardation on the london-van der waals forces. *Phys. Rev.*, 73:360–372, Feb 1948. doi: 10.1103/PhysRev.73.360. URL <https://link.aps.org/doi/10.1103/PhysRev.73.360>.
- [3] Carlos Farina. The Casimir effect: some aspects. *Brazilian Journal of Physics*, 36:1137 – 1149, 12 2006. ISSN 0103-9733.
- [4] Wolfgang P. Schleich. *Quantum Optics in Phase Space*. Wiley-VCH, Berlin, 2001.
- [5] W.M.R. Simpson and U. Leonhardt. *Forces of the Quantum Vacuum: An Introduction to Casimir Physics*. World Scientific Publishing Company Pte Limited, 2015. ISBN 9789814644778.
- [6] M. Bordag, G. L. Klimchitskaya, U. Mohideen, and V. M. Mostepanenko. Advances in the Casimir effect. *Int. Ser. Monogr. Phys.*, 145:1–768, 2009.
- [7] J. Mehra. Temperature correction to the casimir effect. *Physica*, 37(1):145 – 152, 1967. ISSN 0031-8914.
- [8] J. Blocki, J. Randrup, W.J. Świątecki, and C.F. Tsang. Proximity forces. *Annals of Physics*, 105(2):427 – 462, 1977. ISSN 0003-4916.
- [9] M. Maggiore. *A Modern Introduction to Quantum Field Theory*. EBSCO ebook academic collection. Oxford University Press, 2005. ISBN 9780198520733.
- [10] Tom Lancaster and Stephen J Blundell. *Quantum field theory for the gifted amateur*. Oxford University Press, Oxford, Apr 2014.

-
- [11] M.E. Peskin and D.V. Schroeder. *An Introduction to Quantum Field Theory*. Advanced book classics. Avalon Publishing, 1995. ISBN 9780201503975.
- [12] Steven K Lamoreaux. The casimir force: background, experiments, and applications. *Reports on progress in Physics*, 68(1):201, 2004.
- [13] Lowell S. Brown and G. Jordan Maclay. Vacuum stress between conducting plates: An image solution. *Phys. Rev.*, 184:1272–1279, Aug 1969.
- [14] Julian Schwinger, Lester L DeRaad, and Kimball A Milton. Casimir effect in dielectrics. *Annals of Physics*, 115(1):1 – 23, 1978. ISSN 0003-4916.